Plant Physiology and Biochemistry 63 (2013) 39–48

Contents lists available at SciVerse ScienceDirect

Plant Physiology and Biochemistry

journal homepage: www.elsevier.com/locate/plaphy

Research article

Plastidial NADP-malic enzymes from grasses: Unraveling the way to the C_4 specific isoforms

Mariana Saigo*, Clarisa E. Alvarez, Carlos S. Andreo, María F. Drincovich

Centro de Estudios Fotosintéticos y Bioquímicos (CEFOBI), Universidad Nacional de Rosario, Suipacha 531, Rosario 2000, Argentina

ARTICLE INFO

Article history:
Received 21 August 2012
Accepted 6 November 2012
Available online 24 November 2012

Keywords:
C_4 photosynthesis
NADP-malic enzyme
Maize
Sorghum
Rice
Structure–function relationship

ABSTRACT

Malic enzyme is present in many plant cell compartments such as plastids, cytosol and mitochondria. Particularly relevant is the plastidial isoform that participates in the C_4 cycle providing CO_2 to RuBisCO in C_4 species. This type of photosynthesis is more frequent among grasses where anatomical preconditioning would have facilitated the evolution of the C_4 syndrome. In maize (C_4 grass), the photosynthetic NADP dependent Malic enzyme (ZmC_4-NADP-ME, L-malate:NADP oxidoreductase, E.C. 1.1.1.40) and the closest related non-photosynthetic isoform (Zm*non*C_4-NADP-ME, L-malate:NADP oxidoreductase, E.C. 1.1.1.40) are both plastidial but differ in expression pattern, kinetics and structure. Features like high catalytic efficiency, inhibition by high malate concentration at pH 7.0, redox modulation and tetramerization are characteristic of the photosynthetic NADP-ME. In this work, the proteins encoded by sorghum (C_4 grass) and rice (C_3 grass) NADP-ME genes, orthologues of the plastidial NADP-MEs from maize, were recombinantly expressed, purified and characterized. In a global comparison, we could identify a small group of residues which may explain the special features of C_4 enzymes. Overall, the present work presents biochemical and molecular data that helps to elucidate the changes that took place in the evolution of C_4 NADP-ME in grasses.

1. Introduction

Maize (*Zea mays*) and sorghum (*Sorghum bicolor*) are very important crops for human and cattle feeding and are becoming valuable feedstock for biofuels and new generation plastics [4,28]. They are classified as C_4 as they perform this highly efficient photosynthesis by concentrating CO_2 in the vicinity of RuBisCO. Maize and sorghum belong to the most widespread subtype of C_4 photosynthesis, where the CO_2 is mainly provided by the decarboxylation of malate by the NADP dependent malic enzyme (NADP-ME). Both species belong to the Andropogoneae tribe and diverged approximately 13 million years ago (Mya) [1]. The CO_2 decline that occurred 35–25 Mya promoted the evolution of C_4 photosynthesis in grasses [6,33]. Then, several biochemical and anatomical modifications were necessary to originate the C_4 metabolism, including the specialization of already existing enzymes by the re-localization and change of functional properties [32,33]. Whole genome and segmental duplications during maize and sorghum evolution gave rise to multiple copies that facilitated the recruitment of already existing genes to meet their new roles in photosynthesis [35,29,3].

Malic enzyme is represented by a multi-member family of plastidial, cytosolic and mitochondrial isoforms in maize [11,9,12,34,24]. The enzyme that participates in the C_4 cycle (ZmC_4-NADP-ME, L-malate:NADP oxidoreductase, E.C. 1.1.1.40, *nadpme-IVc* gene named by Christin et al. [7]) and the closest related *non*C_4 isoform (Zm*non*C_4-NADP-ME, L-malate:NADP oxidoreductase, E.C. 1.1.1.40, *nadpme-IVa* gene named by Christin et al. [7]) are both plastidial but differ in expression pattern, kinetics and structure. The photosynthetic enzyme is inhibited by high malate concentrations at pH 7.0 and assembles as tetramers, but the non-photosynthetic isoform is not inhibited by malate and assembles as dimers [11,9,34]. Moreover, ZmC_4-NADP-ME activity, but not Zm*non*C_4-NADP-ME activity, is redox-modulated [2].

In this work, naturally occurring variants of photosynthetic and non-photosynthetic plastidial NADP-MEs from grasses were compared to find out features specific for the enzymes, which may be associated to regions and/or residues in the primary structure that were adapted during the evolution. Thus, the products of sorghum and rice (*Oryza sativa*) NADP-ME genes, orthologues of the plastidial NADP-MEs from maize, were expressed and characterized, comparing their main kinetic and structural features. As

Abbreviations: DTT, dithiothreitol; IBZ, iodosobenzoate; NADP-ME, NADP-malic enzyme; ZmC_4-NADP-ME, maize photosynthetic NADP-ME; Zm*non*C_4-NADP-ME, maize non-photosynthetic plastidial NADP-ME.

* Corresponding author. Tel.: +54 341 4371955; fax: +54 314 4370044.
E-mail address: saigo@cefobi-conicet.gov.ar (M. Saigo).

0981-9428/$ – see front matter © 2012 Elsevier Masson SAS. All rights reserved.
http://dx.doi.org/10.1016/j.plaphy.2012.11.009

a result, several differences were detected between the C_4 and the *non*C_4 enzymes, identifying a small group of residues which may be linked to the special features of C_4 enzymes. Besides, the plastidial NADP-ME from rice shares characteristics, as well as key residues, with both the C_4 and the *non*C_4 sorghum and maize enzymes. Overall, the present work sheds light on the way of C_4 NADP-ME evolution in grasses.

2. Results

2.1. Identification of plastidial NADP-MEs from sorghum and comparison to maize and rice plastidial NADP-MEs

In order to identify plastidial NADP-MEs from sorghum, a blast search in the genome database (www.phytozome.net, [29,18]) was performed using the maize plastidial NADP-MEs [11,34]. The products of the genes Sb03g003230 (*nadpme-IVc* [7]) and Sb09g017550 (*nadpme-IVa* [7]), referred to in this work as SbC_4-NADP-ME (L-malate:NADP oxidoreductase, E.C. 1.1.1.40) and Sb*non*C_4-NADP-ME (L-malate:NADP oxidoreductase, E.C. 1.1.1.40), were the most similar to the plastidial NADP-MEs from maize ZmC_4-NADP-ME (J05130, *nadpme-IVc* [7]) and Zm*non*C_4-NADP-ME (AY315822, *nadpme-IVa* [7]), respectively. The genomic flanking sequences of the genes in sorghum were analyzed and compared to the flanking genes of maize plastidial NADP-ME genes (Fig. 1a). Particularly in the case of sorghum, a gene encoding a third plastidial NADP-ME was located upstream Sb03g003230 gene (Sb03g003220, *nadpme-IVb* [7]) (Fig. 1a).

A phylogenetic analysis of mature plastidial NADP-MEs from sorghum, maize and rice (OschlME, L-malate:NADP oxidoreductase, E.C. 1.1.1.40 [5]) in comparison to the already characterized NADP-MEs from *Arabidopsis* was also performed [17, fig. 1b]. Both the genomic flanking sequences analysis and the phylogenetic relationships detected (Fig. 1a and b) indicate that ZmC_4- and SbC_4-NADP-ME are orthologues genes; as well as Zm*non*C_4- and Sb*non*C_4-NADP-ME. These observations are in accordance with the genomic and phylogenetic studies of Wang et al. [38] and Christin et al. [7].

Due to the scarce information about the functional relevance of NADP-ME genes in sorghum, the relative abundance of the transcripts encoded by *SbC_4-NADP-ME* and *Sb*non*C_4-NADP-ME* was compared in leaves, sheaths and roots of sorghum seedlings by qRT-PCR. *SbC_4-NADP-ME* was the most abundant in leaves and was underrepresented in sheaths and roots (Fig. 1c), in accordance to

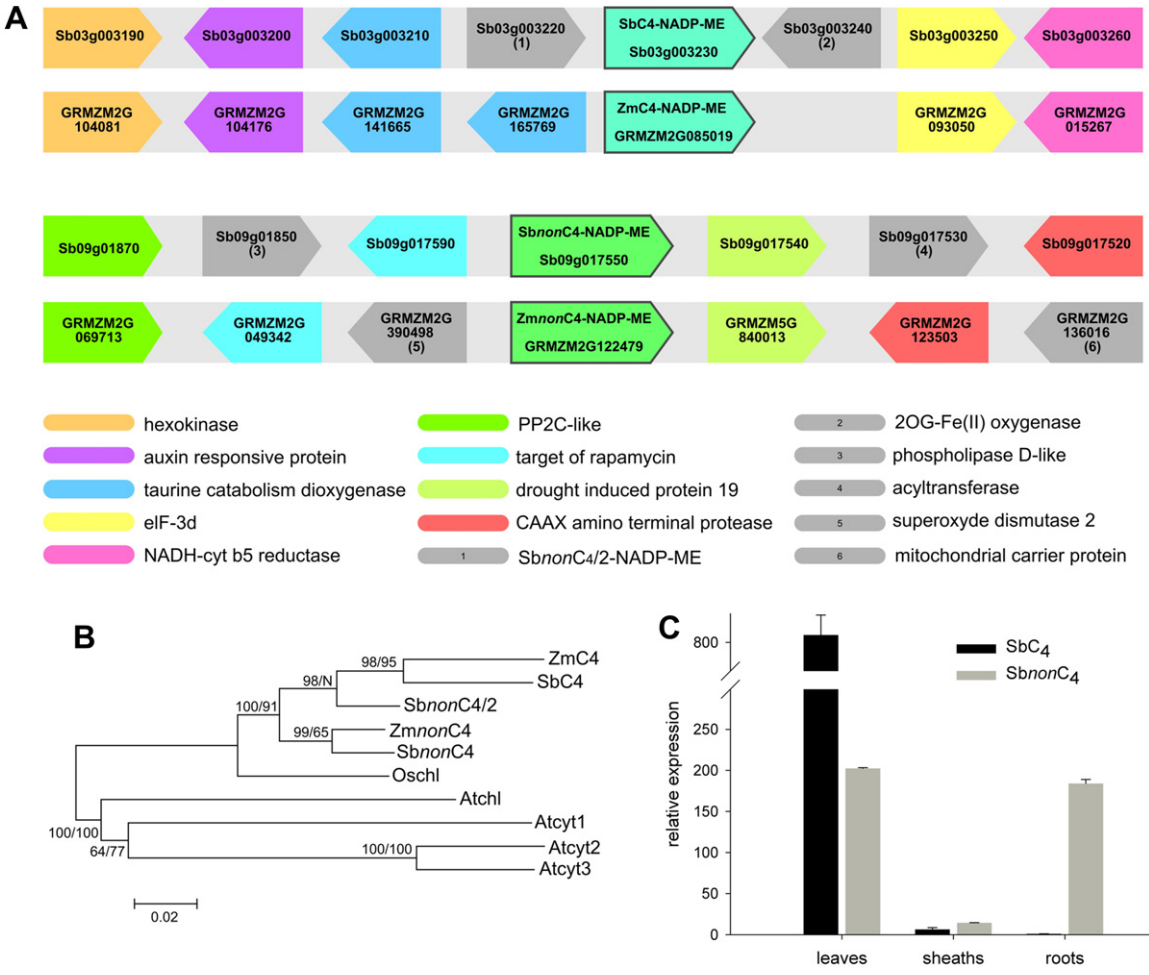

Fig. 1. Plastidial NADP-MEs genes from sorghum. (A) Flanking genes of plastidial NADP-ME genes in sorghum and maize. Arrows with the same color indicate genes with the same putative function. Genes in gray do not have orthologues in the regions analyzed. Genes ID derived from sequencing projects are indicated in each case (Phytozome v8.0, 29). (B) Phylogenetic tree comparing mature NADP-MEs from sorghum, maize, rice and Arabidopsis. Bootstrap values from neighbor-joining and maximum parsimony (NJ/MP) analyses are shown next to branches. Zm indicates *Zea mays*, Sb indicates *Sorghum bicolor*, Os indicates *Oryza sativa* and At indicates *Arabidopsis thaliana*. AtchI corresponds to a plastidial isoform and Atcyt1- to -3 correspond to cytosolic isoforms [16]. (C) Relative abundance of transcripts of SbC_4-NADP-ME and Sb*non*C_4-NADP-ME in three different sorghum organs. The transcripts were analyzed by qRT-PCR and normalized to *actin1* gene expression. Values of relative expression are the means +/− SD of at least three different measurements. (For interpretation of the references to colour in this figure legend, the reader is referred to the web version of this article.)

the photosynthetic role of the encoded protein previously reported by Christin et al. [7] and Wang et al. [38].

On the other hand, *SbnonC$_4$-NADP-ME* was predominant in sheaths and roots (Fig. 1c). This pattern of expression is also comparable to the one displayed by the orthologues from maize [34]. The relative abundance of the transcript of Sb03g003220 gene (Fig. 1a and b) was also analyzed (not shown); however, its level of expression was very low in all the organs tested in comparison to *SbC$_4$-NADP-ME* and *SbnonC$_4$-NADP-ME* (Fig. 1c). These results suggest that Sb03g003220 may represent a genomic duplication of Sb03g003230 not found in maize which functionality is unknown.

The cDNAs obtained from total mRNA from sorghum seedlings were used as templates to amplify the full-length sequences of *SbC$_4$-NADP-ME* and *SbnonC$_4$-NADP-ME*. In order to include a plastidial NADP-ME from a C_3 grass, the cDNA corresponding to the rice plastidial NADP-ME [5] was also cloned and referred to as *OschlME* in this work (Fig. 1b). The predicted protein sequences of plastidial sorghum, maize and rice NADP-MEs were compared, showing a high degree of identity among all proteins, ranging from 81 to 93% (Fig. 2). Several conserved regions, such as sites I–V described in plant NADP-MEs [13] are found in all the aligned sequences (Fig. 2). Sites I–IV contain some of the residues essential for catalysis in human NAD(P)-ME [39] and sites II and V contribute to the conformation of the NADP-binding site [13,10] (Fig. 2).

2.2. Cloning and recombinant expression of mature plastidial NADP-MEs from sorghum, maize and rice

In order to proceed with the biochemical characterization of the plastidial NADP-MEs, recombinant enzymes were expressed in *Escherichia coli* and purified. The transit peptide processing site of ZmC$_4$-NADP-ME was *in silico* predicted between positions 61 and 62, which were corroborated by sequencing of the protein purified from maize leaves [26]. Unfortunately, this approach was unsuccessful with Zm*non*C$_4$-NADP-ME due to the low yield of the purification from maize roots [26]. In previous works with this enzyme, the mature recombinant enzyme was obtained considering the cleavage site between residues 40 and 41 predicted *in silico* [34,9]. Nevertheless, recent results indicate that the transit peptide is processed *in vivo* near the residue analogous to number 62 of ZmC$_4$-NADP-ME (unpublished results). Then, for this work, Zm*non*C$_4$-NADP-ME, SbC$_4$-NADP-ME, Sb*non*C$_4$-NADP-ME and OschlME were cloned and expressed starting at the residue analogous to number 62 of ZmC$_4$-NADP-ME (position indicated with a black arrow in Fig. 2), as was performed with ZmC$_4$-NADP-ME [11]. All the purified proteins, after removal of the N-terminal tag, showed molecular masses between 62 and 64 kDa, as deduced by SDS-PAGE and cross reacted with anti-Zm*non*C$_4$-NADP-ME antibodies (not shown).

2.3. Kinetic characterization of sorghum plastidial NADP-MEs and comparison to maize plastidial isoforms

The kinetic characterization of the sorghum plastidial NADP-MEs was performed at pH 8.0 (Table 1); 7.0 and 6.5 (Table 2). At pH 8.0, sorghum plastidic NADP-MEs displayed typical Michaelis–Menten kinetics for both malate and NADP. At this pH, the sorghum photosynthetic NADP-ME (SbC$_4$-NADP-ME) displayed significant higher catalytic efficiencies for both NADP and malate than the non-photosynthetic counterpart (Sb*non*C$_4$-NADP-ME, Table 1). This is also verified when comparing maize photosynthetic and non-photosynthetic NADP-MEs (Table 1), as previously indicated [9].

At pH 7.0, SbC$_4$-NADP-ME displayed substrate inhibition at concentrations higher than 3 mM malate (Fig. 3a), which was also previously described for ZmC$_4$-NADP-ME [9]. On the other hand, in the case of Zm*non*C$_4$- and Sb*non*C$_4$-NADP-ME, weak malate inhibition was observed at pH 7.0 (Fig. 3a). In order to compare the kinetic parameters and malate inhibition among the NADP-MEs, the kinetic model assuming two malate binding sites that describes ZmC$_4$-NADP-ME response at pH 7.0 was applied [9]. Based on this model, k_{cat}, K_C and the parameters describing malate inhibition (K_R and φ) were estimated for the photosynthetic and non-photosynthetic NADP-MEs from maize and sorghum at pH 7.0 (Table 2). At pH 7.0, the photosynthetic NADP-MEs from maize and sorghum displayed higher k_{cat} and malate affinity (lower K_C) than the non-photosynthetic counterparts, presenting significant higher catalytic efficiencies (Table 2). Regarding malate inhibition, stronger inhibition would be characterized by both higher malate affinity to the allosteric site (lower K_R) and lower φ, which is the k_{cat} ratio of the enzyme with and without malate bound at the allosteric site [9]. Thus, to further depict the malate inhibition phenomenon, it would be useful to calculate the product of $K_R \times \varphi$, which would be lower when the inhibition is stronger (Table 2). When comparing these parameters between the photosynthetic and non-photosynthetic NADP-MEs from maize and sorghum, higher malate inhibition is observed for the photosynthetic enzymes (lower $K_R \times \varphi$, Table 2).

When maize and sorghum isoforms were assayed at pH 6.5 at varying malate concentration, the four NADP-MEs showed substrate inhibition when malate concentration increased. Moreover, at this pH, the enzymes were more efficiently inhibited by malate than at pH 7.0, as shown by a lower K_R, φ or both (Table 2). Again, as observed at pH 7.0, stronger malate inhibition is shown by the photosynthetic NADP-MEs than by the non-photosynthetic counterparts (Table 2). This kinetic pH-dependent behavior can be visualized in the K_R versus φ plot (Fig. 3b), in which there can be recognized three concentric regions: at pH 6.5 all enzymes near the origin (very strong malate inhibition), surrounded by ZmC$_4$- and SbC$_4$-ME at pH 7.0 (strong malate inhibition) and finally, more distant, Zm*non*C$_4$- and Sb*non*C$_4$-at pH 7.0 (weak malate inhibition) (Fig. 3b).

2.4. Kinetic studies of plastidial rice NADP-ME

Kinetic parameters of the plastidial NADP-ME from the C_3 grass rice (OschlME) display similarities with both C_4 and *non*C$_4$ enzymes. At pH 8.0, k_{cat}, $S_{0.5}$ of NADP, K_m of malate and malate catalytic efficiency ($k_{cat} \cdot K_C^{-1}$) resemble those of *non*C$_4$ enzymes (Table 1), while at pH 7.0 k_{cat}, K_R and φ are more similar to the parameters of C_4 enzymes (Table 2). In this sense, at pH 7.0 OschlME is located near ZmC$_4$- and SbC$_4$-NADP-ME in the K_R versus φ plot (Fig. 3b).

2.5. Redox modulation of recombinant SbC$_4$-, SbnonC$_4$-NADP-ME and OschlME

In a recent work, redox activity modulation was observed for maize photosynthetic NADP-ME isoform (ZmC$_4$-NADP-ME), but the kinetic response of Zm*non*C$_4$-NADP-ME was insensitive to changes of the redox conditions [2]. In order to analyze this modulation in other plastidial NADP-MEs, purified recombinants SbC$_4$-, Sb*non*C$_4$-NADP-ME, and OschlME were incubated with chemical oxidants (Fig. 4). Three different oxidants that differ in their redox potentials were used: diamide, iodosobenzoate (IBZ) and $CuCl_2$. The results show a time-dependent decrease of SbC$_4$-NADP-ME activity in the presence of the three oxidants, reaching nearly 80% of initial activity with $CuCl_2$ and 70% with diamide and IBZ at 80 min (Fig. 4). On the contrary, neither Sb*non*C$_4$-NADP-ME nor OschlME displayed significant activity variation by incubation with any chemical oxidant, at least up to 80 min of incubation (Fig. 4). In order to assess the reversal of SbC$_4$-NADP-ME oxidation, the enzyme was

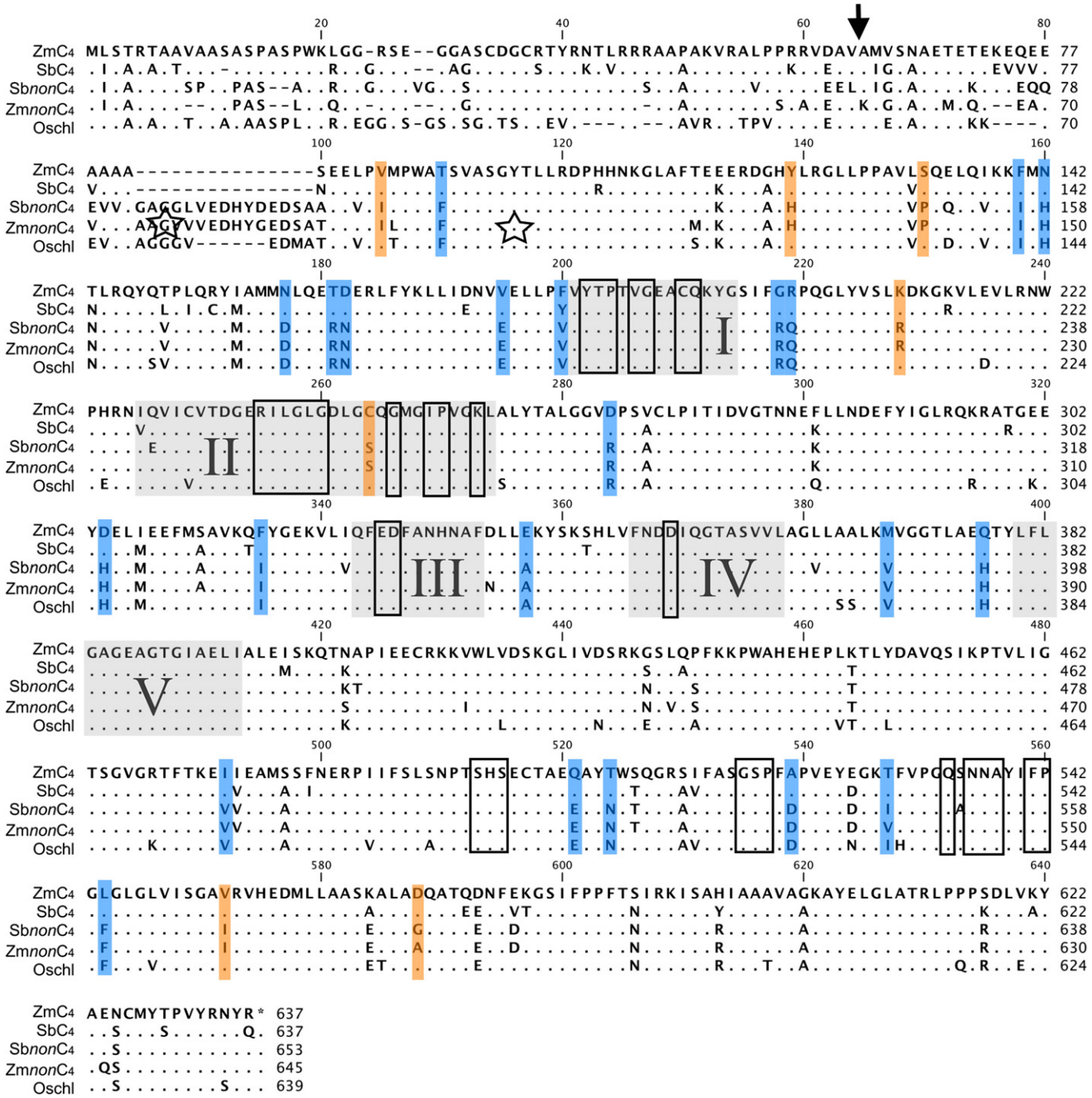

Fig. 2. Amino acid sequence alignment of plastidial NADP-MEs from maize, sorghum and rice. Plant conservative sites I–V are highlighted in gray [13]. Essential residues for catalysis are enclosed in black rectangles [39]. The black arrow indicates the transit peptide processing site of ZmC$_4$-NADP-ME [26]. Residues conserved in C$_4$ NADP-MEs from maize and sorghum that differ from the *non*C$_4$ NADP-MEs are highlighted in orange (when the corresponding residues of Oschl are identical to C$_4$ NADP-MEs) or blue (when the corresponding residues of Oschl are identical to *non*C$_4$ NADP-MEs). Stars indicate the starting residues of DelN1 and DelN2 in Zm*non*C$_4$-NADP-ME. Consensus residue number (top of the figure) and the number of amino acid residues of each sequence (right on the figure) are present in order to guide any search in this alignment. (For interpretation of the references to colour in this figure legend, the reader is referred to the web version of this article.)

incubated with diamide for 60 min (approximately 65% of initial activity), desalted, and further incubated with the reductant dithiothreitol (DTT). In the presence of DTT, a complete restore of the initial NADP-ME activity was observed after 90 min of incubation (data not shown). Thus, photosynthetic sorghum and maize NADP-MEs [2] display redox activity modulation, which is not observed in the case of the non-photosynthetic counterparts and OschlME.

2.6. Quaternary structure of plastidial NADP-MEs from grasses

Previous work showed that the quaternary conformations preferentially adopted by recombinant ZmC$_4$- and Zm*non*C$_4$-NADP-ME were tetramers and dimers, respectively [11,34]. The native molecular masses of both proteins were calculated by size-exclusion chromatography and correlated with data obtained by non-denaturing electrophoresis. Here, we assessed the quaternary

Table 1
Kinetic parameters of recombinant maize, sorghum and rice plastidial NADP-MEs at pH 8.0. The indicated kinetic parameters are the mean average of at least three separate determinations, using at least two different preparations of each enzyme. Values are given as average ± standard deviation.

	k_{cat} (s^{-1})	K_m malate (mM)	$k_{cat} \cdot K_m$ malate^{-1} (s^{-1} mM^{-1})	K_m NADP (μM)	$k_{cat} \cdot K_m$ NADP^{-1} (s^{-1} μM^{-1})
ZmC_4	198.9 ± 2.4	0.19 ± 0.01	1046.9	8.0 ± 0.3	61.2
Zm*non*C_4	158.1 ± 3.4	0.78 ± 0.08	202.6	70.2 ± 3.2	2.7
SbC_4	275.7 ± 3.4	0.36 ± 0.03	765.7	11.0 ± 1.1	27.9
Sb*non*C_4	158.8 ± 2.0	0.62 ± 0.03	256.0	16.8 ± 1.4	10.2
Oschl	181.6 ± 3.7	0.81 ± 0.07	224.1	35.0 ± 2.7 (n_H: 1.4 ± 0.1)	5.8

n_H: Hill parameter *n*.

Table 2
Kinetic parameters of recombinant maize, sorghum and rice plastidial NADP-MEs at pH 7.0 and pH 6.5. The indicated kinetic parameters are the mean average of at least three separate determinations, using at least two different preparations of each enzyme. Values are given as average ± standard deviation.

	pH	k_{cat} (s^{-1})	K_C malate (mM)	$k_{cat} \cdot K_C^{-1}$ (s^{-1} mM^{-1})	K_R malate (mM)	φ	$K_R \cdot \varphi$ (mM)
ZmC_4	7	264.5 ± 16.7	0.30 ± 0.04	881.6	2.1 ± 0.5	0.33 ± 0.02	0.69
	6.5	319.6 ± 24.8	0.21 ± 0.06	1521.8	0.3 ± 0.1	0.04 ± 0.01	0.01
Zm*non*C_4	7	187.7 ± 8.2	0.52 ± 0.05	361.1	31.5 ± 24.7	0.16 ± 0.34	5.04
	6.5	92.8 ± 5.4	0.21 ± 0.04	442.0	3.9 ± 1.3	0.09 ± 0.06	0.35
SbC_4	7	282.5 ± 16.6	0.20 ± 0.03	1412.7	16.8 ± 10.0	0.17 ± 0.19	2.86
	6.5	199.6 ± 18.7	0.10 ± 0.02	2100.9	1.0 ± 0.3	0.005 ± 0.002	0.01
Sb*non*C_4	7	197.9 ± 13.3	0.67 ± 0.14	295.5	5.7 ± 5.7	0.62 ± 0.08	3.53
	6.5	210.8 ± 30.9	1.82 ± 0.53	117.0	6.3 ± 3.7	0.13 ± 0.07	0.82
Oschl	7	361.4 ± 135.0	2.32 ± 1.23	155.0	0.6 ± 0.5	0.34 ± 0.12	0.19
	6.5	162.2 ± 9.9	0.55 ± 0.1	294.8	3.2 ± 0.92	0.14 ± 0.02	0.45

conformations of the recombinant NADP-MEs by non-denaturing electrophoresis followed by western blotting and NADP-ME activity staining. First, we confirmed that the shorter version of Zm*non*C_4-NADP-ME constructed in this work migrates as dimers (Fig. 5a). SbC_4-NADP-ME displayed two bands that were immunodetected by anti-ZmC_4-NADP-ME. Their migrations were consistent with dimers and tetramers, but only the tetrameric form was active under the activity staining conditions (Fig. 5a). Sb*non*C_4-NADP-ME showed a pattern similar to Zm*non*C_4-NADP-ME, for which the catalytically active dimers are the preferred conformation adopted (Fig. 5a). On the other hand, OschlME showed a unique band of an intermediate migration between C_4 and *non*C_4 enzymes visualized by the immunodetection and activity staining (Fig. 5a).

2.7. N-terminal divergence in plastidial NADP-MEs from grasses

The plastidial NADP-MEs characterized in this work mostly differ in the N-terminal region of the mature proteins sequences (Fig. 2). Remarkably, Zm*non*C_4-NADP-ME, Sb*non*C_4-NADP-ME and OschlME have insertions of 9–15 residues, between residues 81 and 82 of ZmC_4-NADP-ME (Fig. 2). To assess whether the length of this region had any effect on the catalytic and structural features, two truncated versions of Zm*non*C_4-NADP-ME, DelN1 and DelN2 that lack the first 20 and 45 residues (Fig. 2), were constructed and characterized.

The kinetic responses of DelN1 to malate at pH 8.0 and pH 7.0 were not modified in comparison to Zm*non*C_4-NADP-ME (not shown); however the mobility exhibited by DelN1 in non-

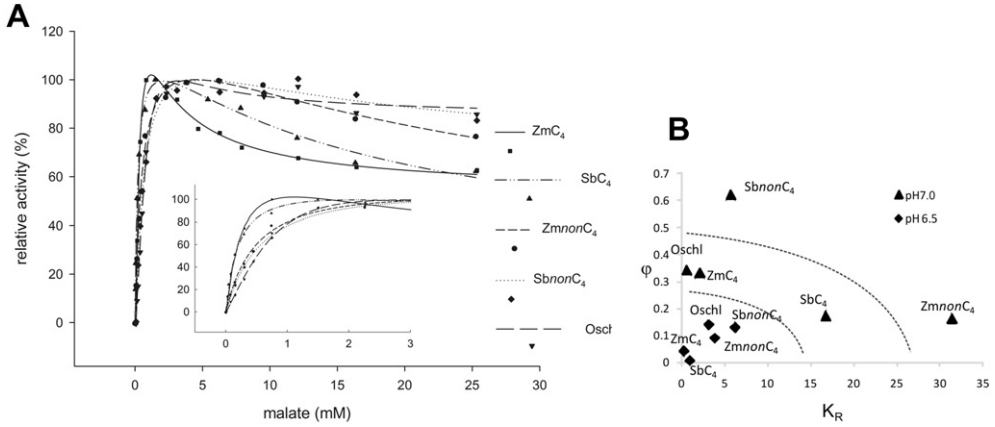

Fig. 3. (A) Kinetics of plastidic NADP-MEs from sorghum, maize and rice at pH 7.0 at varying malate concentration. Initial rates of malate oxidative decarboxilation of ZmC_4-NADP-ME, Zm*non*C_4-NADP-ME, SbC_4-NADP-ME, Sb*non*C_4-NADP-ME and OschlME are presented as % of maximal activity as a function of free malate concentration. Assay conditions were 100 mM Tris–HCl pH 7.0, 10 mM Mg^{2+} and 0.5 mM NADP. The inset shows the catalytic responses at low malate concentrations. (B) Strength of malate inhibition in plastidial NADP-MEs. The parameters that define the malate inhibition mechanism (K_R and φ) estimated at pH 6.5 (◆) and 7.0 (▲) (Table 2) were plotted for rice and sorghum and maize photosynthetic and non-photosynthetic NADP-MEs. Three different areas, from higher to lower malate inhibition, are indicated in the plot.

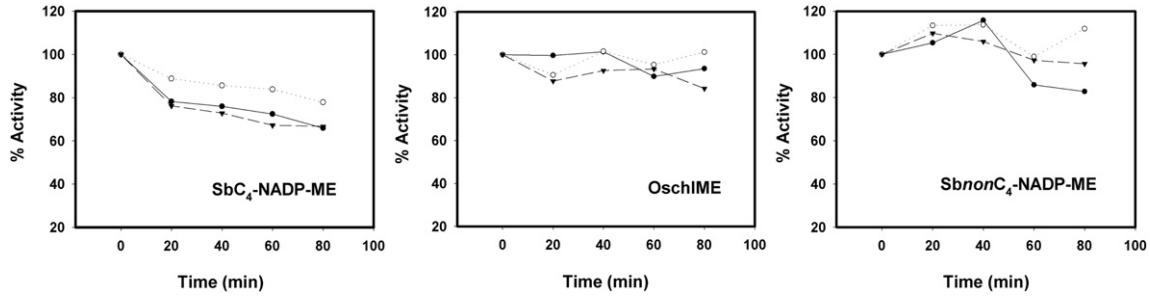

Fig. 4. Redox-modulation of recombinant sorghum and rice plastidic NADP-MEs. Recombinant Oschl-ME, SbC_4-NADP-ME and Sb*non*C_4-NADP-ME were incubated with either 1 mM IBZ (●), 5 mM diamide (▼) or 25 μM $CuCl_2$ (○). At several times, NADP-ME activity was measured and expressed as the % of initial activity. Typical results are shown from at least three different incubations of each enzyme using different preparations.

denaturing electrophoresis changed to the mobility observed by ZmC_4-NADP-ME (tetramer) (Fig. 5b). The deletion of a larger extension in the N-terminal region of Zm*non*C_4-NADP-ME (DelN2) resulted in a loss of activity probably due to a misfolding of the protein as deduced from the aggregation observed in non-denaturing electrophoresis (data not shown).

3. Discussion

3.1. Functional conservation of maize and sorghum NADP-ME orthologues

The biochemical properties and expression patterns of plastidial NADP-ME of different C_4 species are closely connected with the role of each isoform. While the enzymes involved in C_4 photosynthetic process, ZmC_4 and SbC_4, are abundant in leaves and display malate inhibition at pH 7.0 (Fig. 6), the plastidial non photosynthetic counterparts, Zm*non*C_4 and Sb*non*C_4, are mainly detected in roots and do not show malate regulation (Fig. 6). Structural similarities also have been found between these enzymes: SbC_4 and ZmC_4 assemble mainly as tetramers and Sb*non*C_4 and Zm*non*C_4 as dimers (Fig. 6). Furthermore, the redox regulation recently reported for ZmC_4-NADP-ME [2] was also detected for SbC_4-NADP-ME (Fig. 6). All these data show that the sequence conservation between orthologues resulted in conserved protein structures that determined conserved kinetic features, to fulfill similar roles. While ZmC_4 and SbC_4 are implicated in C_4 photosynthesis, Zm*non*C_4 and Sb*non*C_4 are implicated in non-photosynthetic processes such as house-keeping functions and response to plant defense inducers [13,27,34].

3.2. Light/dark regulation of maize and sorghum malic enzymes

In relation to the photosynthetic role of C_4-NADP-ME isoforms, it is crucial for these enzymes to provide high amounts of carbon dioxide to fixation under light conditions. Avoiding the over-consumption of malate during the night is also important to prevent a carbon starvation condition, as found in *Arabidopsis* [14,41]. Several studies have shown that maize photosynthetic ME have two main ways to achieve a fine-tuning regulation of the activity by light/dark transition: the decrease of the activity as stromal pH decreases in the night and the redox regulation in accordance with the day/night redox status. The high malate concentration observed in plant tissues [15] and the decrease in pH observed in chloroplast in darkness, both produce a decrease in NADP-ME activity when carbon fixation is not active. When assayed in all sorghum and maize isoforms, malate inhibition phenomenon was detected in all enzymes but at different pH. Thus, the inhibition could be assigned to a residue or group of residues which functionality to malate binding and/or inhibition mechanism depends on the pH. Ionizable residues which could meet these requirements were not found in protein sequences analyzed here (Fig. 2). Then, most probably, malate inhibition relies on conserved residue/s which K of ionization is different in C_4 and *non*C_4 enzymes. The evolution of the high performance of C_4 enzymes at pH 8.0 was accompanied by a high efficiency at pH 7.0 as well. To avoid the negative impact of this high activity at pH 7.0 (dark condition), the photosynthetic isoforms could have evolved the mechanism of malate inhibition. Since OschlME is negatively regulated by high malate at pH 7.0 but the kinetic performance is low compared to C_4 enzymes (see below), the inhibition mechanism in C_4 enzymes could have evolved previously to kinetic improvement so that high activity at neutral pH was prevented. The detection of the phenomenon of malate inhibition in all plastidial isoforms at pH 6.5 clearly shows that the structural bases exist in all enzymes but are evident at different pH, indicating that the evolution of the inhibition at pH 7.0 would have been an easy road. There are only seven residues that are conserved among C_4-NADP-ME and OschlME, which could play an important role in the malate inhibition

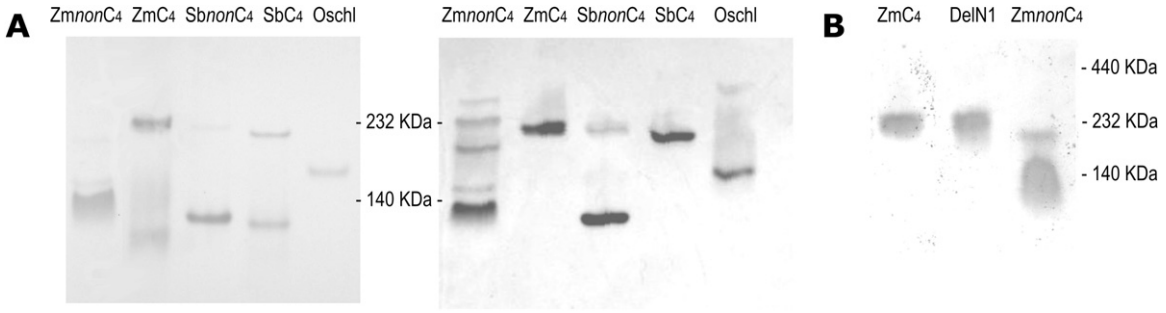

Fig. 5. Native PAGE of plastidial NADP-MEs. Recombinant NADP-MEs (500 ng of each protein) were loaded in 6% polyacrylamide gels. (A) The proteins were detected by western blotting (left panel) and NADP-ME activity staining (right panel). Numbers between panels indicate the migration of native molecular marker. (B) Native PAGE of DelN1 in comparison with Zm*non*C_4- and ZmC_4-NADP-ME. The proteins were detected by activity staining. Numbers on the right side indicate the migration of native molecular marker.

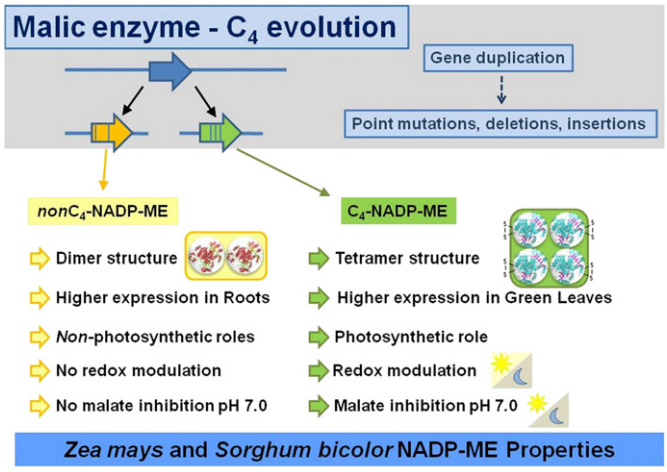

Fig. 6. Summary of the differences between photosynthetic and non-photosynthetic plastidial NADP-MEs from maize and sorghum.

mechanism at pH 7.0 (Fig. 2, orange boxes). Although further studies are needed to elucidate the contribution of each residue, the approach used in the present work allowed the identification of a few number of residues that may be important in the acquisition of the malate inhibition mechanism.

Furthermore, in this work it was found a correlation in the evolution of the redox-modulation in C_4-MEs from maize and sorghum. Accordingly, the cysteine residues in positions 192, 246, 270 and 410, implicated in the redox modulation of ZmC_4-NADP-ME [2], are conserved in SbC_4-NADP-ME and explain the redox response of this isoform (Fig. 2). On the other hand, the replacement of Cys 246 to Ser in Zm*non*C_4-NADP-ME and Sb*non*C_4-NADP-ME (Fig. 2) may be responsible for the lack of redox-modulation (Fig. 4).

3.3. Structure conservation among plastidial NADP-MEs from C_4 species

For ZmC_4-NADP-ME and SbC_4-NADP-ME it was possible to detect the presence of inactive dimers coexisting with tetramers. This fact and previously reported evidence with purified NADP-MEs from other species [20,36], support the model of C_4-ME tetramer as a dimer of dimers, as was confirmed for human, *Ascaris suum* and pigeon MEs crystal structures [39,8,40]. On the other hand, maize and sorghum *non*C_4 enzymes are unable to form tetramers. This could be due to a structural impediment that avoids the proper interaction between dimers and/or the lack of the affinity sites that drive the tetramerization. In this paper, the deletion of an N-terminal segment of Zm*non*C_4-NADP-ME induced the change from a dimeric to a tetrameric structure. Then, it is straightforward to deduce that this region prevents the tetramer formation and that the sites of dimers interaction are present in Zm*non*C_4-NADP-ME. Since for photosynthetic ME of other sources the transition of dimers to tetramers was accompanied by a rise in the catalytic efficiency [21,36], it could be possible to increase the kinetic performance of *non*C_4 MEs by inducing the tetramerization. Nevertheless, the deletion-induced tetramerization did not change the main kinetic features of this enzyme, supporting the idea that the structural determinants for high kinetic efficiency are absent in Zm*non*C_4-NADP-ME. In relation to the structure of OschlME, the predicted molecular mass did not agree with the formation of dimers nor tetramers. Given that this observation was verified by gel filtration chromatography (not shown), OschlME could be assembling as dimers but structurally different from Zm*non*C_4 and Sb*non*C_4.

3.4. Rice plastidial NADP-malic enzyme regulation

The catalytic efficiency of OschlME is as low as for *non*C_4 sorghum and maize isoforms but it responds negatively to high malate at pH 7.0 as C_4 enzymes. Considering that rice is a C_3 species, the mechanism of malate inhibition at pH 7.0 could have evolved in OschlME in relation to its roles in rice, which have been suggested to be related to the supplying of carbon and reducing power for amino acid biosynthesis, counterbalance of ion uptake in roots, among others [5]. Recently, it has been reported that a unique chloroplastic PEPC provides organic acids for ammonia assimilation, which is crucial for rice to survive in reductive environments such as waterlogged soils [25]. The kinetics of this enzyme was similar to that of the C_4 PEPC, including a better performance under illumination due to a decrease in the sensitivity to malate inhibition. In this context, OschlME could help in such metabolism converting malate into pyruvate in the plastids to provide carbon skeletons and reducing power for ammonia assimilation or other diurnal metabolism. In relation to redox regulation, OschlME does not display changes in its activity in oxidative or reductive conditions, as was seen for Sb*non*C_4 and Zm*non*C_4. This could be due to the existence of Val instead of Cys at position 231, which was one of the residues implicated in the redox control of ZmC_4-NADP-ME (Fig. 2). The engineering of a redox sensitive NADP-ME in chloroplasts has not been considered in rice molecular breeding projects and represents an interesting issue to be explored.

3.5. The origin of photosynthetic NADP-MEs

Several genomic and phylogenetic analyses show that the C_4 pathway has evolved several times in grasses [1,33]. In relation to this, some preconditioning elements found in the ancestors of the different C_4 lineages, such as structural characteristics, predisposal of gene duplications, among others, have probably facilitated the acquisition of the C_4 pathway [33]. Gene duplications and subsequent modifications were essential in the evolution of new C_4 elements [38,33]. In the tribe Andropogoneae, the existence of three copies of plastidial NADP-ME genes, as in the case of sorghum, would be explained by two events of duplication of the ancestral gene [7]. The presence of C_4 and *non*C_4 genes in sorghum and maize could be the result of a process of duplication of an ancestral C_4 or *non*C_4 NADP-ME possibly followed by subfuntionalisation and finally neo-funtionalisation [7,31]. In any case, the evolutionary products were isoforms well different in their biochemical characteristics that support their current roles.

The alignment of protein sequences shows that 448 residues are strictly conserved among the plastidial enzymes here studied (Fig. 2). These include the amino acids involved in substrates binding and catalysis. In 29 positions, the residues were identical in C_4 group and *non*C_4 group, but different from each other (Fig. 2 blue and orange boxes). These residues could be the most important in the C_4-NADP-MEs evolution because their conservation indicates that they are functionally relevant but have different consequences in each NADP-ME group. Among the 29 residues mentioned above, the residues 284, 450 and 539 (Fig. 2) were found by Christin et al. [7] under positive selection during the evolution of C_4-NADP-ME in grasses, suggesting that they might be the most important to explain the kinetical and structural differences studied in this work. In this sense, the product of Sb03g003220 (nadpme-IVb) could be interesting to characterize given that residue 450 in this protein is conserved in C_4-NADP-ME while the residues 284 and 539 are

conserved in *non*C_4-NADP-ME. Another approach to correlate the biochemical characteristics with specific residues would be analyzing the impact of their replacements in mutant proteins obtained by site-directed mutagenesis.

4. Methods

4.1. Search and analysis of NADP-ME sequences

The known sequences of plastidial NADP-MEs from maize and rice were: ZmC_4-NADP-ME (J05130), Zm*non*C_4-NADP-ME (AY315822) and OschlME (D16499). Plastidial NADP-MEs of sorghum were identified by blast search in genome databases [Phytozome v8.0, [29,18]] using maize sequences. The phylogenetic analyses were performed by neighbor-joining and maximum parsimony methods in MEGA4 software [37]. The gene colinearity was inferred by identifying the homologous genes between the flanking genes of plastidial NADP-MEs from maize and sorghum [Phytozome v8.0, [18]]. The alignment of protein sequences was performed with the software CLC sequence viewer v6.5.4 (CLC bio A/S).

4.2. Plant material

Sorghum (*S. bicolor* (L) Moench) and rice (*Oryza sativa var. japonica*) plants were grown in a growing chamber under a 12 h-light/12 h-dark regime at a photosynthetically active photon flux density (PPFD) of 300 μmol quanta m^{-2} s^{-1}. For qRT-PCR experiments, three different segments of 10 days sorghum seedlings we selected: fully expanded leaves, a middle region mostly composed by sheaths and developing leaves (referred as "sheaths" in the text) and roots.

4.3. RNA extraction and cDNA synthesis

Total RNA was isolated from 100 mg of green leaves of rice and leaves, sheaths and roots of sorghum seedlings using the Trizol reagent (Gibco-BRL) following the instructions of the manufacturer. The concentration and integrity of the preparations were assayed by agarose 2% gel electrophoresis. Two micrograms of total RNA was reverse transcribed with Superscript II Reverse Transcriptase (Invitrogen) using oligodT as primer. The cDNAs were used as templates for cloning and quantitative PCR assays.

4.4. Quantitative real-time PCR analysis

Relative gene expression was determined by quantitative real-time PCR (qRT-PCR) on a Mx3000P detection system and the MxPro – Mx3005P software version 4.01 (Stratagene). Primers were designed using RealTime PCR SciTool web tool (Integrated DNA Technologies, http://www.idtdna.com/scitools/Applications/RealTimePCR/) to allow for amplification of 70–100 bp products of similar GC and Tm characteristics. The generation of specific PCR products was confirmed by melting curve, gel analysis and PCR amplification using plasmids containing cDNAs of SbC_4-NADP-ME and Sb*non*C_4-NADP-ME as templates. The PCR mix contained SYBR® Green I 1× (Invitrogen), 2.5 mM $MgCl_2$, 0.5 μM of each primer, 0.05 U/μl Platinum Taq and 1× buffer provided by the manufacturer (Invitrogen). Tenfold dilutions of the cDNAs synthesized as described above from different sorghum tissues were used as templates. Thermal cycling parameters were as follows: initial denaturation at 94 °C for 2 min and 40 cycles of 10 s at 96 °C, 15 s at 56 °C and 35 s at 72 °C. The *actin1* gene was used as reference. Relative gene expression was calculated using a modified version of the comparative $2^{-\Delta\Delta}C_T$ method [30], the efficiencies were calculated as described by Liu and Saint [23] and the error propagation according to Ref. [19]. The oligonucleotide primers pairs used for SbC_4-NADP-ME, Sb*non*C_4-NADP-ME and *actin1* amplification were: SbC_4-for: CCCAC CCTTCACCAACATC, SbC_4-rev: GCATATGCCACCAGGTCTTTG, Sb*non*C_4-for: CTCTGCATATTTCACCAGGTCTCTT, Sb*non*C_4-rev: CTCTGCATATTTCACCAGGTCTCTT, Act1-for: CAACTGGGACGATATGGAGAAG, Act1-rev: TGGGCGGAAAGAATTAGAAGC.

4.5. Cloning of full length cDNA of NADP-malic enzymes from maize, sorghum and rice

The cDNAs of rice leaves and a mixture of cDNAs from leaves, sheaths and roots of sorghum seedlings were used as templates. The primers used for SbC_4 amplification were: SbC_4-sacI (GTGGAGGAGCTCGCGATAGGCT) and SbC_4-xhoI (CTCGAGCTACTGGTAGTTACGGTA), for Sb*non*C_4 were: Sb*non*C_4-sacI and Sb*non*C_4-xhoI (CTCGAGCAGCAGCACTATCGGTAA) and for Oschl were: Oschl-salI (GTCGACGCGATGGAGTCCG) and Oschl-xhoI (CTCGAGGCGGCGTTACCG). In the case of Zm*non*C_4-NADP-ME, the template was a plasmid constructed previously [34] and the primers were: Zm*non*C_4-ecorV (GATATCGCCGCGGAGATGGAGCAG) and Zm*non*C_4-xhoI (CTCGAGCTACCGGTAGTTACGGT). In all cases the amplified fragments codify the proteins without transit peptides. The nucleotides underlined indicate restriction sites used for subcloning into pET32 expression vector. PCR conditions were: initial denaturation at 94 °C for 5 min followed by 35 cycles of 94 °C 30 s, 58 °C 1 min, 72 °C 3 min, and a final elongation step at 72 °C for 5 min. The amplified products were cloned into pGEMT-Easy (Promega) and the sequences were verified by automated sequencing. Finally, the cDNAs corresponding to the mature MEs were subcloned into pET32 downstream of an inducible T7 promoter system (Novagen).

4.6. Cloning of DelN1 and DelN2

DelN1 was constructed amplifying a fragment of Zm*non*C_4-NADP-ME with the PCR primers delN1-ndeI and (5′-GGCGTCCATATGGAGGACCACT-3′) Zm*non*C_4-xhoI (5′-CTCGAGCTACCGGTAGTTACGGT-3′). The nucleotides underlined indicate restriction sites used for subcloning into pET28 expression vector. PCR conditions were: initial denaturation at 94 °C for 5 min followed by 35 cycles of 94 °C 30 s, 58 °C 1 min, 72 °C 3 min, and a final elongation step at 72 °C for 5 min. The amplified products were cloned into pGEMT-Easy (Promega) and the sequences were verified by automated sequencing. DelN2 was obtained subcloning the BamHI-XhoI fragment of Zm*non*C_4-NADP-ME (from 306 to 1935 of AY315822) in pET32. The sequences of the truncated proteins are indicated in Fig. 2.

4.7. Preparation of recombinant MEs

Protein synthesis inductions and purifications were performed as previously described for maize NADP-MEs [11,34] with minor modifications. Briefly, the expression vectors were transformed into *E. coli* BL21 cells for enzymes over-expression. Expressions of NADP-MEs were induced with 10% lactose and the cells were incubated at 16 °C overnight. After induction, cells were centrifuged at 6000 g at 4 °C for 15 min and resuspended in buffer A (100 mM Tris–HCl pH 8.0, 10 mM $MgCl_2$, 2 mM PMSF, 5 μg/μl DNase I). The lysate obtained by sonication was centrifuged at 15,000 g at 4 °C for 20 min and the supernatant was mixed with binding buffer 8× and glycerol to reach 1× and 10% concentrations, resp. Ni-NTA affinity column (Qiagen) was equilibrated with Binding buffer (5 mM imidazole, 500 mM NaCl, 20 mM Tris–HCl pH

7.9) and then loaded with the lysate. After washing with Binding and Wash (49 mM imidazole, 500 mM NaCl, 20 mM Tris–HCl pH 7.9) buffers the proteins were eluted with Elute buffer (200 mM imidazole, 500 mM NaCl, 20 mM Tris–HCl pH 7.9). The purified enzymes were then buffer-exchanged and concentrated in buffer TM (100 mM Tris–HCl pH 8.0, 10 mM $MgCl_2$) by a centrifugal filter device (Amicon Ultra-15, Millipore). Purified fusion NADP-ME proteins were then incubated with Enterokinase (1 μg protein:0.05 U enterokinase) in the buffer supplied by the manufacturer (EKmax, Invitrogen) at 16 °C for 2 h to remove the N-terminus encoded in the expression vector. Since DelN1 was cloned in pET28, the N-terminal fusion was removed incubating the protein with the restriction protease Thrombin (5:1 w/w, ICN) in buffer TM 10% glycerol, at 16 °C for 2 h. The purity and integrity of the proteins obtained were examined by SDS-PAGE and the concentrations were estimated using the Bradford method and the absorbance at 280 nm.

4.8. Enzyme kinetic analysis

NADP-ME activity was determined spectrophotometrically as previously described [11]. Initial velocity studies were performed by varying the concentration of one of the substrates while keeping the concentration of the other substrates at saturating levels. Kinetic parameters were calculated at least by triplicate determinations and subjected to non-linear regression. All substrate concentrations reported refer to the free, uncomplexed, reactant concentrations and were calculated considering the dissociation constant of the different complexes formed (Mg^{2+}-NADP or Mg^{2+}-malate). When analyzing the inhibition of NADP-ME by high malate concentration, the equation model that was used to fit kinetic data was that described in Detarsio et al. [9]:

$$v = V_{\max}\frac{M/K_C + \varphi M^2/K_C K_R}{1 + M/K_C + M/K_R + M^2/K_C K_R}$$

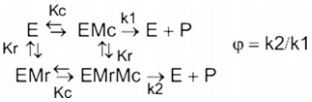

In this kinetic scheme, K_C is the dissociation constant of the malate bound to the catalytic binding site and K_R is the dissociation constant of the malate bound to the regulatory allosteric site. The catalytic constants k_1 and k_2 correspond to product formation when the allosteric site is empty or occupied, respectively. φ is the ratio of k_2 and k_1. This last value should be less than 1, as the activity when the allosteric site is occupied is lower than when it is empty. When no inhibition by high substrate concentration was found, the kinetic data obtained were fit to typical Michaelis–Menten or Hill equations. All data fitting work was carried out using the program Sigma Plot 11.0 (Jandel).

4.9. Redox-modulation of recombinant NADP-MEs activity

The different purified recombinant NADP-MEs (approximately 50 μg) were incubated in a buffer containing 100 mM Tris–HCl and 10 mM $MgCl_2$ (pH 8.0) for 2 h at 0 °C with 10 mM Dithiothreitol (DTT) to complete reduction of their –SH residues and dialyzed. At different time intervals of incubation at 0 °C with different redox compounds (1 mM Iodosobenzoate (IBZ); 25 μM $CuCl_2$; 5 mM diamide or 10 mM Dithiothreitol (DTT)), aliquots were withdrawn and assayed for NADP-ME activity. The modification of the recombinant enzymes was stopped by at least 100-fold dilution of the redox compounds in the assay media. No significant decrease in activity was found when the recombinant NADP-MEs were incubated in the absence of the redox compounds. The addition of the redox compounds (100-fold diluted) to the NADP-ME assay medium had no significant effect on the enzyme activity assay.

4.10. Gel electrophoresis

Non-denaturing PAGE was performed in 6% (w/v) polyacrylamide gels according to Ref. [22]. Proteins were visualized with Coomassie Blue, electroblotted onto a nitrocellulose membrane for immunodetection or assayed for malic enzyme activity as described in Ref. [34]. Bound antibodies were located with alkaline phosphatase-conjugated goat anti-rabbit IgG according to the manufacturer's instructions (Sigma). The electrophoresis was run at 150 V and 10 °C.

Accession numbers: Sequence data from this article can be obtained in the EMBL/Genbank data libraries under accession number: JQ905099.

Acknowledgments

This work was supported by Agencia Nacional de Promoción Científica y Tecnológica (PICT 2164 and PICT 733, Argentina) and Consejo Nacional de Investigaciones Científicas y Técnicas (CONICET, Argentina). CSA; MFD and MS are members of the Researcher Career of CONICET and CEA is a fellow of the same institution.

References

[1] S. Aliscioni, H.L. Bell, G. Besnard, P.-A. Christin, J.T. Columbus, M.R. Duvall, E.J. Edwards, L. Giussani, K. Hasenstab-Lehman, K. Hilu, T.R. Hodkinson, A.L. Ingram, E.A. Kellogg, S. Mashayekhi, O. Morrone, C.P. Osborne, N. Salamin, E. Spriggs, S.A. Smith, F. Zuloaga, New grass phylogeny resolves deep evolutionary relationships and discovers C_4 origins, New Phytol. 193 (2012) 304–312.

[2] C.E. Alvarez, E. Detarsio, S. Moreno, C.S. Andreo, M.F. Drincovich, Functional characterization of residues involved in redox modulation in maize photosynthetic NADP-malic enzyme activity, Plant Cell Physiol. 53 (2012) 1144–1153.

[3] S. Aubry, N.J. Brown, J.M. Hibberd, The role of proteins in C_3 plants prior to their recruitment into the C_4 pathway, J. Exp. Bot. 62 (2011) 3049–3059.

[4] N.C. Carpita, M.C. McCann, Maize and sorghum: genetic resources for bioenergy grasses, Trends Plant Sci. 13 (2008) 415–420.

[5] W. Chi, J. Yang, N. Wu, F. Zhang, Four rice genes encoding NADP malic enzyme exhibit distinct expression profiles, Biosci. Biotechnol. Biochem. 68 (2004) 1865–1874.

[6] P.-A. Christin, G. Besnard, E. Samaritani, M.R. Duvall, T.R. Hodkinson, V. Savolainen, N. Salamin, Oligocene CO_2 decline promoted C_4 photosynthesis in grasses, Curr. Biol. 18 (2008) 37–43.

[7] P.-A. Christin, E. Samaritani, B. Petitpierre, N. Salamin, G. Besnard, Evolutionary insights on C_4 photosynthetic subtypes in grasses from genomics and phylogenetic, Genome Biol. Evol. 1 (2009) 221–230.

[8] D.E. Coleman, G.S.J. Rao, E.J. Goldsmith, P.F. Cook, B.G. Harris, Crystal structure of the malic enzyme from *Ascaris suum* complexed with nicotinamide adenine dinucleotide at 2.3 Å resolution, Biochemistry 41 (2002) 6928–6938.

[9] E. Detarsio, C.E. Alvarez, M. Saigo, C.S. Andreo, M.F. Drincovich, Identification of domains involved in tetramerization and malate inhibition of maize C_4-NADP-malic enzyme, J. Biol. Chem. 282 (2007) 6053–6060.

[10] E. Detarsio, C.S. Andreo, M.F. Drincovich, Basic residues play key roles in catalysis and NADP(+)-specificity in maize (*Zea mays* L.) photosynthetic NADP(+)-dependent malic enzyme, Biochem. J. 382 (2004) 1025–1030.

[11] E. Detarsio, M. Gerrard Wheeler, M.V. Campos Bermúdez, C.S. Andreo, M.F. Drincovich, Maize C_4 NADP-malic enzyme: expression in *E. coli* and characterization of site-directed mutants at the putative nucleotide binding sites, J. Biol. Chem. 278 (2003) 13757–13764.

[12] E. Detarsio, V.G. Maurino, C.E. Alvarez, G.L. Müller, C.S. Andreo, M.F. Drincovich, Maize cytosolic NADP-malic enzyme (ZmCytNADP-ME): a phylogenetically distant isoform specifically expressed in embryo and emerging roots, Plant Mol. Biol. 68 (2008) 355–367.

[13] M.F. Drincovich, P. Casati, C.S. Andreo, NADP-malic enzyme from plants: a ubiquitous enzyme involved in different metabolic pathways, FEBS Lett 490 (2001) 1–6.

[14] H. Fahnenstich, M. Saigo, M. Niessen, M.I. Zanor, C.S. Andreo, A.R. Fernie, M.F. Drincovich, U. Flügge, V.G. Maurino, Alteration of organic acid

metabolism in Arabidopsis overexpressing the maize C_4 NADP-malic enzyme causes accelerated senescence during extended darkness, Plant Physiol. 145 (2007) 640–652.
[15] L.E. Fridlyand, J.E. Backhausen, R. Scheibe, Flux control of the malate valve in leaf cells, Arch. Biochem. Biophys. 349 (1998) 290–298.
[16] M.C. Gerrard Wheeler, C.L. Arias, M.A. Tronconi, V.G. Maurino, C.S. Andreo, M.F. Drincovich, *Arabidopsis thaliana* NADP-malic enzyme isoforms: high degree of identity but clearly distinct properties, Plant Mol. Biol. 67 (2008) 231–242.
[17] M.C. Gerrard Wheeler, M.A. Tronconi, M.F. Drincovich, C.S. Andreo, U. Flügge, V.G. Maurino, A comprehensive analysis of the NADP-malic enzyme gene family of Arabidopsis, Plant Physiol. 139 (2005) 39–51.
[18] D.M. Goodstein, S. Shu, R. Howson, R. Neupane, R.D. Hayes, J. Fazo, T. Mitros, W. Dirks, U. Hellsten, N. Putnam, D.S. Rokhsar, Phytozome: a comparative platform for green plant genomics, Nucleic Acids Res. 40 (D1) (2012) D1178–D1186.
[19] J. Hellemans, G. Mortier, A. De Paepe, F. Speleman, J. Vandesompele, qBase relative quantification framework and software for management and automated analysis of real-time quantitative PCR data, Genome Biol. 8 (2007) R19.
[20] A.A. Iglesias, C.S. Andreo, Kinetic and structural properties of NADP-malic enzyme from sugarcane leaves, Plant Physiol. 92 (1990a) 66–72.
[21] A.A. Iglesias, C.S. Andreo, NADP-dependent malate dehydrogenase (decarboxylating) from sugar cane leaves, Eur. J. Biochem. 733 (1990b) 729–733.
[22] U.K. Laemmli, Cleavage of structural proteins during the assembly of the head of bacteriophage T4, Nature 227 (1970) 680–685.
[23] W. Liu, D.A. Saint, New quantitative method of real time reverse transcription polymerase chain reaction assay based on simulation of polymerase chain reaction kinetics, Anal. Biochem. 302 (2002) 52–59.
[24] A. Maier, M.B. Zell, V.G. Maurino, Malate decarboxylases: evolution and roles of NAD(P)-ME isoforms in species performing C_4 and C_3 photosynthesis, J. Exp. Bot. 62 (2011) 3061–3069.
[25] C. Masumoto, S.-I. Miyazawa, H. Ohkawa, T. Fukuda, Y. Taniguchi, S. Murayama, M. Kusano, K. Saito, H. Fukayama, M. Miyao, Phosphoenolpyruvate carboxylase intrinsically located in the chloroplast of rice plays a crucial role in ammonium assimilation, Proc. Natl. Acad. Sci. U. S. A. 107 (2010) 5226–5231.
[26] V.G. Maurino, M.F. Drincovich, C.S. Andreo, NADP-malic enzyme isoforms in maize leaves, Biochem. Mol. Biol. Int. 38 (1996) 239–250.
[27] V.G. Maurino, M. Saigo, C.S. Andreo, M.F. Drincovich, Non-photosynthetic malic enzyme from maize: a constitutively expressed enzyme that responds to plant defense inducers, Plant Mol. Biol. 45 (2001) 409–420.
[28] B.P. Mooney, The second green revolution? Production of plant-based biodegradable plastics, Biochem. J. 418 (2009) 219–232.
[29] A.H. Paterson, J.E. Bowers, R. Bruggmann, I. Dubchak, J. Grimwood, H. Gundlach, G. Haberer, The *Sorghum bicolor* genome and the diversification of grasses, Nature 457 (2009) 551–556.
[30] M.W. Pfaffl, A new mathematical model for relative quantification in real-time RT-PCR, Nucleic Acids Res. 29 (2001) e45.
[31] P. Rondeau, C. Rouch, G. Besnard, NADP-malate dehydrogenase gene evolution in Andropogoneae (Poaceae): gene duplication followed by sub-functionalization, Ann. Bot. 96 (2005) 1307–1314.
[32] R.F. Sage, The evolution of C_4 photosynthesis, New Phytol. 161 (2004) 341–370.
[33] R.F. Sage, T.L. Sage, F. Kocacinar, Photorespiration and the evolution of C(4) photosynthesis, Annu. Rev. Plant Biol. 63 (2012) 19–47.
[34] M. Saigo, F.P. Bologna, V.G. Maurino, E. Detarsio, C.S. Andreo, M.F. Drincovich, Maize recombinant *non*C_4 NADP-malic enzyme: a novel dimeric malic enzyme with high specific activity, Plant Mol. Biol. 55 (2004) 97–107.
[35] P.S. Schnable, D. Ware, R.S. Fulton, J.C. Stein, F. Wei, S. Pasternak, C. Liang, The B73 maize genome: complexity, diversity, and dynamics, Science 326 (2009) 1112–1115.
[36] C.P. Spampinato, P. Casati, C.S. Andreo, Factors affecting the oligomeric state of NADP-malic enzyme from maize and wheat tissues: a chemical crosslinking study, Biochim. Biophys. Acta 1383 (1998) 245–252.
[37] K. Tamura, J. Dudley, M. Nei, M.S. Kumar, MEGA4: molecular evolutionary genetics analysis (MEGA) software version 4.0, Mol. Biol. Evol. 24 (2007) 1596–1599.
[38] X. Wang, U. Gowik, H. Tang, J.E. Bowers, P. Westhoff, A.H. Paterson, Comparative genomic analysis of C_4 photosynthetic pathway evolution in grasses, Genome Biol. 10 (6) (2009) 68.
[39] Y. Xu, G. Bhargava, H. Wu, G. Loeber, L. Tong, Crystal structure of human mitochondrial NAD(P)(+)-dependent malic enzyme: a new class of oxidative decarboxylases, Structure 7 (1999) 877–889.
[40] Z. Yang, H. Zhang, H. Hung, C. Kuo, L. Tsai, H.S. Yuan, W. Chou, G. Chang, L. Tong, Structural studies of the pigeon cytosolic NADP+-dependent malic enzyme, Prot. Sci. 11 (2002) 332–341.
[41] M.B. Zell, H. Fahnenstich, A. Maier, M. Saigo, E.V. Voznesenskaya, G.E. Edwards, C.S. Andreo, F. Schleifenbaum, C. Zell, M.F. Drincovich, V.G. Maurino, Analysis of Arabidopsis with highly reduced levels of malate and fumarate sheds light on the role of these organic acids as storage carbon molecules, Plant Physiol. 152 (2010) 1251–1262.